Time transfer by laser link (T2L2): characterization and calibration of the flight instrument

2014 Metrologia 51 503

(http://iopscience.iop.org/0026-1394/51/5/503)

OPEN ACCESS
IOP Publishing | Bureau International des Poids et Mesures Metrologia
Metrologia **51** (2014) 503–515 doi:10.1088/0026-1394/51/5/503

Time transfer by laser link (T2L2): characterization and calibration of the flight instrument

E Samain[1], P Vrancken[2], P Guillemot[3], P Fridelance[4] and P Exertier[1]

[1] GeoAzur—Observatoire de la Côte d'Azur, 2130 route de l'Observatoire, 06460 Caussols, France
[2] DLR—German Aerospace Center, Oberpfaffenhofen, 82234 Weßling, Germany
[3] CNES—French Space Agency, 18 av Edouard Belin, 31400 Toulouse, France
[4] Phusipus Intégration, 8 Allée Bellevue, Saint Vallier de Thiey, France

E-mail: etienne.samain@oca.eu

Received 8 April 2014, revised 26 June 2014
Accepted for publication 7 July 2014
Published 19 August 2014

Abstract
The T2L2 project (time transfer by laser link) allows for the synchronization of remote ultra-stable clocks over intercontinental distances (Fridelance *et al* 1997 *Exp. Astron.* **7**, Samain and Fridelance 1998 *Metrologia* **35** 151–9). The principle is derived from satellite laser ranging technology with dedicated space equipment designed to record arrival times of laser pulses at the satellite. The space segment has been launched in June 2008 as a passenger experiment on the ocean altimetry satellite Jason 2. T2L2 had been specified to yield a time stability of better than 1 ps over 1000 s integration time and an accuracy of better than 100 ps. This level of performance requires a rigorous data processing which can be performed only with a comprehensive calibration model of the whole instrumentation. For this purpose, several experimental measurements have been performed before and during the integration phase of the T2L2 space instrument. This instrument model is one of the cornerstones of the data reduction process which is carried out to translate the raw information to a usable picosecond time transfer. After providing a global synopsis of the T2L2 space instrument, the paper gives a description of the experimental setup for the instrument characterization. It then details the different contributions within the calibration model and concludes with an applied example of a space to ground time transfer.

Keywords: time transfer, clocks, photodetection, event timer, laser, laser ranging

(Some figures may appear in colour only in the online journal)

1. Introduction

T2L2 is a time transfer technique based on the propagation of light pulses between clocks to be synchronized [1, 2]. It is based on a ground segment materialized by a ground station network, issued from the satellite laser ranging station network, and a dedicated space instrument which was launched as a passenger experiment on the Jason 2 satellite in June 2008 [3, 4]. The elementary T2L2 time transfer is made between a given laser station and the space instrument. For a ground time transfer between two or more laser stations, several independent elementary links are established and the space segment is only used as a relay between ground clocks. Each ground clock has to be connected with a laser station. The laser station emits asynchronous short light pulses (some picoseconds) towards the satellite. The station measures the start time of every pulse. An optical laser ranging reflector array on-board the satellite returns a part of the light pulse to the ground station so that the ground station can record the return time after reflection from space and compute the time of flight of all the pulses emitted (this is the usual laser ranging technique). The T2L2 payload records, in the time scale of the space oscillator, the light pulses' arrival time on-board. These

data are downloaded to ground with a classical radio link. In principle and to a first approximation, the ground–space time transfer is deduced from the difference between the start time and the arrival time shifted by the time of flight divided by two.

T2L2 was specified to realize time transfers with stability better than 1 ps over 1000 s and accuracy better than 100 ps. These performances are based on the metrology used inside the laser station and also on the T2L2 space instrument [5]. Particular care has been taken during the design and the manufacturing of the instrument to meet these metrological requirements. Two measurement campaigns [6] have been carried out before and during the integration phase of the T2L2 space instrument to the Jason 2 satellite bus to build an accurate model of the instrument. This model is a crucial element for the data reduction process of the space segment which is performed to translate the raw information to a usable picosecond time transfer data set.

The T2L2 space instrument consists of four distinct modules. The first one is the clock which is used as the time reference of the whole T2L2 space instrument, the second one is the event timer permitting to time tag all the events in the timescale of the clock, the third one is the opto-electronic detection module to register and translate the laser events in some electrical events sent to the timer and the last one is the laser ranging array (LRA) to reflect the laser pulses towards the emitting laser station. The clock and the LRA do not belong to the T2L2 assembly itself: the clock is the frequency reference of the DORIS system [7] and the LRA is fundamentally used for the satellite laser ranging system (precise orbit determination).

The optical detection module comprises two photo-detection chains [8]: one of them is working in a non-linear 'Geiger' mode for chronometry, the other one in a linear mode for three distinct purposes: triggering the non-linear detection, measuring the received optical energy and measuring the background light (sunlight backscattered by Earth) [9]. Both detection chains further feature some optical components to optimize the spectral bandwidth and to adjust the field of view of the instrument and the photon number. Each photodetection chain (linear and non-linear) has a distinct optical assembly. The optics of the linear detection are integrated into a single module. The optics of the non-linear detection are divided into two modules coupled by an optical fibre. The primary function of the non-linear photodetection is to generate an electrical pulse from a very low level of light which allows for a timing error as low as possible [10]. The detector used has a significant time-walk dependence on the received energy (typically 20 ps per octave). Several phenomena such as atmospheric turbulence, pointing error and laser energy variation induce tremendous variations of the received energy of up to four orders of magnitude. It is therefore necessary to apply a time compensation of that time walk. This is achieved through the linear photodetector which is able to measure the energy for each received pulse. The energy of each pulse is recorded together with the arrival time finally measured by the event timer and the compensation is applied through a post-processing at ground using a pre-defined model of the time walk.

The on-board clock used by T2L2 is the quartz crystal oscillator of the DORIS instrument [11]. The constraints peculiar to the Jason 2 mission did not allow one to have an atomic clock on-board. Obviously, this configuration presents drawbacks in terms of metrological performances, mainly with respect to the long-term stability and to the accuracy of the oscillator's signal. On the other hand, T2L2 offers the possibility to perform an independent restitution of the oscillator's frequency. This way T2L2 could additionally support the DORIS mission if, as was the case on Jason 1, the excessive sensitivity of the oscillator to the environment (space radiations) came to degrade the localization performances [12].

2. Test benches for the characterization of the T2L2 flight instrument

2.1. Objectives

The exploitation of the whole T2L2 mission relies on the data reduction coming from the ground segment (laser stations) and from the space instrument. The reduction of the ground segment data is performed by the involved laser stations. It takes into account some specifics of each laser station such as internal calibration, time-walk compensation, frequency offset. Apart from the absolute start time of laser pulses which is performed through a dedicated T2L2 calibration procedure, laser station data are directly used without any transformation. The reduction of the space segment data has to be done as an on-ground post-processing using a precise instrumental model of the T2L2 space instrument. Some parts of that model rely on some intrinsic information (geometry of the LRA, distance between LRA and detection, etc) and some parts rely on measurements. This includes for instance the time walk of the detection, transmission of both the linear and non-linear detection versus incident angle or the linearity of the event timer. All the measurements were made during two campaigns with two test benches designed for that purpose [6, 13]. The campaigns were also used to validate the space instrument performances.

2.2. Presentation of the T2L2 test benches

The test benches had been designed to realize six different measurement categories for both instrumental characterization and performance evaluation of all the sub-system of the space instrument.

- Characterization of the time reference and the frequency synthesis of the event timer.
- Event timer modelling and determination of the reduction parameters.
- Optics characterization including geometry, detection dynamic, detection threshold, attitude sensitivity.
- Global chronometry characterization with both optics detection and electrical timing.
- Energy measurement characterization.
- Signal-to-noise ratio determination.

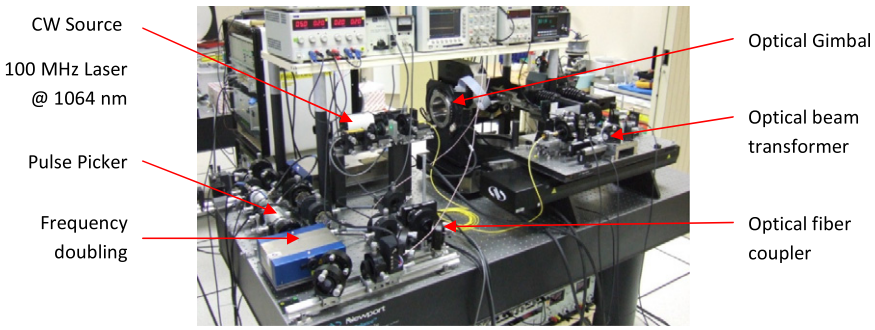

Figure 1. Global test bench during integration at OCA (Observatoire de la Côte d'Azur) facilities used to characterize the T2L2 flight instrument.

The test benches have been designed to basically emulate the whole T2L2 time transfer scheme by providing the laser pulses generated by the laser stations, varying attitude and measurement conditions. Several electronic cabinets control the whole equipment and realize some specific measurements. All the optical elements were integrated on an optical bench which included five distinct modules: pulsed laser, optical beam transformer, optical gimbals, photometry instruments and an optical CW source (figure 1). The electronic cabinets included a single-photon detector, two reference event timers, two atomic clocks and an ultra-stable oscillator used as the global time reference of the whole experiment. The equipment included further an avalanche photodiode used as the optical flux reference and a high-speed PIN photodiode used as a start detector for chronometry reference of the laser pulses.

The electronic cabinets comprised also some specific instruments to power and to control each piece of equipment.

The pulsed laser was a High Q (Austria) picoTRAIN diode-pumped mode-locked laser. The length of the laser resonator was actively controlled by a piezoelectric device for synchronizing the repetition rate on an external frequency source. The cavity provided pulses with 20 ps (FWHM) length with an output power stability better than 1% and a mean power of 0.7 W @ 532.1 nm.

A double pulse picker at the output of the laser permitted to decrease the repetition rate from 100 MHz to arbitrary, selectable rates (as 10 Hz to 1000 Hz). A fraction of the output energy was sent on an InGaAs PIN photodetector to materialize the primary reference of the start time of the laser pulses. The final output energy of the laser-optical system was tuned with a module based on a rotating half-wave plate and a polarizer. This final optical flux was coupled into a single mode optical fibre.

The laser beam was then shaped with an optical module to generate the reference beacons for the space instrument, emulating the incident macroscopic laser pulse at the satellite. From the initial laser, two synchronous beacons were generated, one for the linear channel, the other for the non-linear one. Two different collimators generating two different beam diameters were used in order to adjust the energy density to the specific requirement of each experiment. The module generated two polarized beams separated by the distance corresponding to the distance between the photodetectors of the space instrument. This distance depended on the angle between the main instrument axis and the laser direction. It was adapted by a variable cube corner formed by two plane mirrors at 90° mounted on a translation stage. Each channel included a half-wave plate and a polarizer to adjust the flux.

The optical module gathering the linear detection and the optics of the non-linear photodetection were integrated on a two-axis gimbals permitting to emulate the attitude of the satellite (figure 2). The centre of the non-linear photodetection aperture was located at the cross axes of the gimbals to obtain an invariant time delay whatever the rotation position of the mount.

The energy measurement was realized with a highly sensitive CCD camera (Andor) and a power-meter (Newport). The CCD camera uses a 13.5 µm 2048 × 2048 pixels Marconi CCD42-40 chip. It has a reading noise of 1.6 electrons (RMS) and a quantum efficiency of 0.94 @ 532 nm. The CCD camera was able to give a quantitative information of the received photon number with an accuracy better than 10%. The power-meter has a DC accuracy better than 0.1%.

The single-photon timing reference detector was made with a K14 photodiode [14, 15] coupled with a multi-mode 100/140 µm optical fibre. The photodiode was connected to an active quenching circuit permitting to use the diode in Geiger mode with an active gate of 5 ns.

The reference avalanche photodiode was of the same type as the one in the flight module. It was powered with a stabilized high-voltage source.

The start detector (multi-photon) is made with an InGaAs photodiode FD80IR having a DC bandwidth of 3 GHz.

The two reference event timers (for the emulated station laser pulse start and return) were provided by Dassault Electronique (DE Event timer). Each of them had a repeatability error of 2 ps RMS and a linearity better than 1 ps RMS. They were connected to a common 200 MHz frequency synthesizer slaved to an external 10 MHz reference signal.

The time reference of the experiment was either a signal coming from

- GPS rubidium clock Datum 6000,
- caesium clock HP5071A,
- DORIS EGSE 10 MHz ultra-stable oscillator (EGSE meaning a DORIS engineering model used for the test),
- hydrogen maser (CNES).

This time reference signal was distributed to both the T2L2 event timer and the reference event timers.

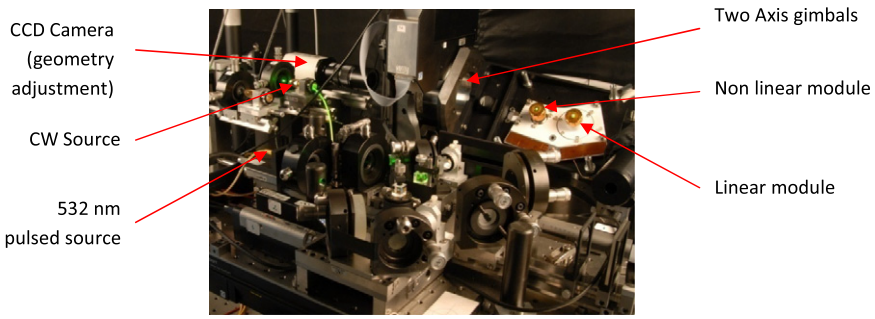

Figure 2. On the right, two-axis gimbals with the optical module of the T2L2 flight model permitting to emulate the attitude of the satellite.

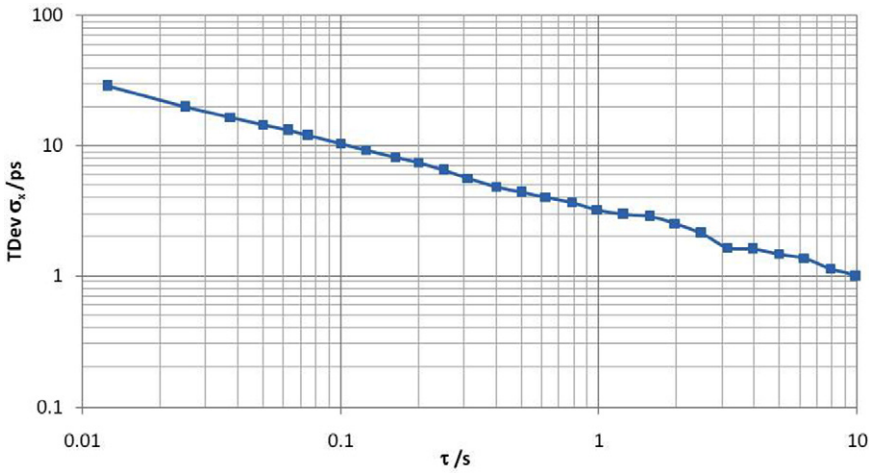

Figure 3. Time stability of a set of 4000 events obtained in a single-photon mode. The result can be fitted by $\sigma_x(\tau) = 3 \times 10^{-12}\tau^{-1/2}$.

The whole measurement project was monitored and controlled by dedicated software, running on a PC, developed by OCA and Phusipus Integration. This software permitted to control each piece of equipment of the test bench and to automate most of the measurement procedures.

2.3. Characterization of the test bench

Several measurements were made to evaluate the main characteristics of the test bench itself [6]. This included some measurements of the reference event timers, of the optical detection modules and of all the optical sources.

The optical pulse width of the picoTRAIN laser was measured with a 20 GHz sampling oscilloscope Tektronics TDS 8200 and a 20 GHz PIN photodiode NewFocus. The pulse width measured was smaller than 25 ps FWHM. The optical contrast between the useful low rate laser pulse and the optical train generated by the laser cavity at the output of the pulse pickers was determined through the computation of the linearity violation as a function of the laser rate. The typical contrast measured is better than 10^{-8}. With a 10 Hz output rate, this contrast permitted to have a useful mean power ten times greater than the rejected train.

Each beam profile was analysed with the Andor CCD camera to quantify the energy flux in front of each aperture of the linear and non-linear detection chain of the space instrument. Each beam was fitted with a Gaussian profile with an error smaller than 2%. The energy of each beacon was measured with the wattmeter at a high repetition rate. The energy flux information together with the profiles permitted to compute the encircled energy in the aperture of each detection channel. The absolute error of the energy was estimated to be better than 30%.

The single-photon repeatability error and the time stability of the whole optical and electrical chain was determined with the picoTRAIN pulse laser, the multi-photon and the single-photon detectors used, respectively, as the start and stop detection and the reference event timers linked to the rubidium clock. Figure 3 shows the time stability of the timing distribution of an ensemble of 4000 laser pulses, emitted at 10 Hz and recorded in single-photon mode.

The repeatability error of the chain in single-photon mode was better than 28 ps RMS and the time stability σ_x (determined as the square root of the time variance) was $3 \times 10^{-12}\tau^{-1/2}$; $\tau_0 = 0.01$ s due to single-photon statistics. In this mode of operation, the most important noise was coming from the single photodetector. This repeatability error and time stability represents the typical performance for that kind of metrology.

The repeatability error of the start detector was determined with the picoTRAIN laser and one of the reference event timers. Both of them were referenced on the clock permitting to realize some measurements in synchronous mode. The overall repeatability error measured was 2.3 ps RMS. This measurement includes the synchronization error of the optical train generation, of the event timer and of the detector.

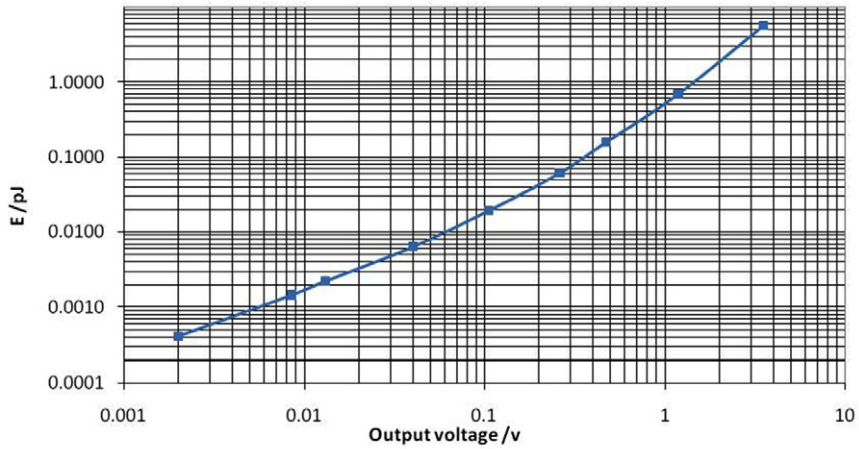

Figure 4. Absolute response of the reference photodiode.

The reference avalanche photodiode was calibrated in a pulsed regime with the picoTRAIN laser to describe the linear output response of the diode as a function of the energy received. This calibration was made with a large Gaussian beam sent alternatively on the reference diode and on the CCD camera. The determination of the energy collected by the sensitive area of the diode was determined with a precise measurement of the beam profile. The result was fitted with a Gaussian profile with an absolute error smaller than 3%. From this fit and from the absolute response of the camera, the absolute energy sent on the reference diode was determined. Figure 4 is an illustration of the absolute response of the reference photodiode.

The energy linearity of the energy control module was determined by computing the difference between the predicted energy set by the rotation position of the half-wave plate and the measured energy made by both the CCD camera and the wattmeter. The thus determined linearity error was better than 0.6% over three orders of magnitude.

The time stabilities of the DORIS EGSE oscillator and the Datum 6000 rubidium clock were measured with one of the reference event timers referenced to the H-maser. The measured time stability of the quartz oscillator alone computed from the square root of the time variance was $1.3 \times 10^{-11} \cdot \tau^{+1/2}$ $\tau_0 = 0.01$ s between 0.01 s and 100 s.

3. Characterization of the T2L2 flight instrument

3.1. Introduction

Two sets of measurements have been conducted to characterize the T2L2 space instrument. The first set has been carried out at the French Space Agency (CNES) centre at Toulouse before integration of the T2L2 instrument on the satellite Jason 2 and the other one at Thales Alenia Space Cannes during the integration phase.

In the first setup, the flight model was integrated on the dedicated test bench (section 2) and connected to a dedicated cabinet (electronic ground support equipment/EGSE) including some power supplies and a communication interface module. The optical part of the flight model was integrated on the two-axes gimbal mount of the test bench. All the measurements were conducted in a class 100 clean room at CNES Toulouse facilities. In the second setup, the T2L2 flight model was integrated in the Jason 2 satellite and connected to the external test bench (providing laser illumination, etc) with two optical fibre-connected collimators for the detection modules. In this latter setup, the position and the orientation of the laser beacon were thus collinear with the main axis of the optics. Most of the measurements were executed with the real DORIS oscillator also integrated in the Jason 2 satellite.

3.2. DORIS local oscillator

The DORIS oscillator is an ultra-stable OCXO's type quartz oscillator developed by the Rakon company [16]. This oscillator was chosen for its metrological performances, both in terms of short-term stability and of sensitivity to external perturbations. In particular, this oscillator uses a dewar structure which allows one to insulate the metrological electronics and the resonator from temperature fluctuations. The lessons learned from Jason 1 [11] also led to the setting-up of a selection process of quartz resonators with respect to their space radiation sensitivity by some sets of measurement of their individual sensitivity.

The oscillator was fully characterized before its integration within the DORIS instrument. Its main performances are summarized in table 1. Considering a typical in-orbit environment, the performance budget is mainly dominated by both thermal and radiation sensitivities.

3.3. T2L2 frequency synthesis

The thermal sensitivity and the time stability of the internal frequency synthesis of the T2L2 flight model was determined by measuring the phase of the 100 MHz output signal with one of the reference event timers. Both the reference event timer and the flight model are driven by the same 10 MHz reference signal. The 100 MHz signal was distributed on a high-speed flip-flop component that was reset by an external signal at a rate of 1 kHz. The reference event timer measures the output

Table 1. Measured performances of the DORIS oscillator: the performance budget is defined by the RMS sum of the different contributors on the frequency slope (over a 12 min sliding window) and the standard deviation of measurements around the slope and is derived from measurements for a typical in-orbit environment. The main contributors are the temperature and the space radiations.

		Performance budget		
Item	Measurement	Slope/min	St. dev.	Comment
Stability (Allan dev. σ_y)	$<3.5 \times 10^{-13}$ from 10 s to 100 s	1.5×10^{-13}	7.9×10^{-13}	2.1 °C peak/100 mn
Ageing	$<1 \times 10^{-11}$/day			
Thermal sensitivity	6.5×10^{-13}/K			
Acceleration sensitivity	$7.6 \times 10^{-10}/g$	7.3×10^{-16}	1.6×10^{-13}	10^{-3} g
Magnetic sensitivity	3.2×10^{-13}/rad	6.3×10^{-15}	3.2×10^{-13}	Magneto Torquer
		4.4×10^{-16}	4.7×10^{-15}	Earth
Radiation sensitivity	6.7×10^{-12}/rad	1.3×10^{-13}	3.1×10^{-12}	1 rad h^{-1} (for 20 mn)
Load sensitivity	$<1.0 \times 10^{-12}$	1.1×10^{-15}	8.3×10^{-16}	0.5 Ω
Power supply sensitivity	$<1.0 \times 10^{-12}$	4.4×10^{-16}	3.3×10^{-16}	10 mV

Table 2. Characteristics of the T2L2 frequency synthesis.

Thermal sensitivity	0.5 ps K^{-1}
Time deviation $\sigma_x = \sqrt{\text{TVAR}}$; $\tau_0 = 0.001$ s	$(0.06 \times 10^{-12}\tau^{-1/2} + 30 \times 10^{-15})$ ps

of that flip-flop as a sequence of consecutive dates. From these dates one computes the modulus (10 ns) to only extract the temporal fluctuation of the 100 MHz as compared with the 10 MHz reference signal. The time stability σ_x is computed by the square root of the time variance of these dates modulo 10 ns. The thermal sensitivity was deduced from the variation of these dates with modulus 10 ns as a function of the temperature of the T2L2 frequency synthesis. For that purpose, the frequency synthesis was operated in a temperature chamber. The results are summarized in table 2.

3.4. Event timer

The event timer permits to get the time stamping of all incoming events in the timescale of the reference oscillator (DORIS). It can be considered as a simple ultra-high speed counter driven by the oscillator. The value of that counter represents the time tag of the event in the time scale of the counter. If the event timer was made with such a simple counter, a temporal resolution in the picosecond range would imply electronic commutation frequencies in the terahertz domain. To avoid that, the timer is made with an analogue vernier and a low-frequency digital counter (100 MHz). The vernier gives the information with a time resolution of 100 fs and a temporal dynamic range of 20 ns while the digital counter has a time resolution of 10 ns and a temporal dynamic range of more than 5 years (54 bits). Both vernier and digital counter are driven by a frequency synthesis module designed to translate the 10 MHz DORIS signal to 100 MHz. The analogue signals used by the vernier are sensitive to temperature fluctuations and ageing. Thus, a dedicated calibration setup is used to monitor their behaviour and to correct their fluctuations during post-processing (figure 5).

Both the digital counter functions and the global control of the timer (digitization, memory, communication, amplitude calibration) are materialized in an FPGA circuit.

The characteristics of the event timer were deduced from a set of measurements using the DE event timer as a reference.

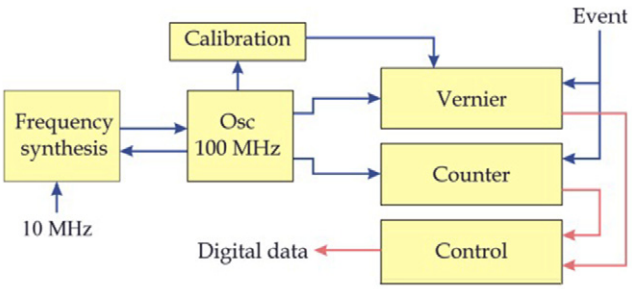

Figure 5. Synoptic of the T2L2 event timer.

The T2L2 and the DE event timers were connected to the same frequency reference. Measurements were conducted with some logical (ECL) events sent simultaneously to both event timers. The analysis is based on the difference x_{diff} between the dates of each event timer. The T2L2 event timer was, for this study, considered as a whole, containing the frequency synthesis, the vernier and the logical counter. The set of measurements permitted to compute the repeatability error, the time stability, the linearity of the vernier and the thermal sensitivity. The repeatability error was obtained by the computation of the quadratic sum of a set of time difference x_{diff} with some random events. Random (or asynchronous) means that there is no temporal correlation between the arrival time of the events and frequency reference of the event timers. Further, the calibration repeatability error was deduced from internal synchronous events generated by the event timer itself. A dedicated setup allowed one to calibrate the timer through the determination of calibration events and the measurement of the harmonics of the internal reference signal for several temperatures. Table 3 summarizes the main characteristics of the T2L2 event timer.

3.5. Detection optics

The non-linear photodetector is based on an avalanche photodiode operating in Geiger mode. The photodiode is gated

Table 3. Characteristics of the T2L2 event timer.

Random event repeatability error (RMS)	2.8 ps
Linearity (RMS)	0.9 ps
Thermal sensitivity	1 ps K^{-1}
Time deviation $\sigma_x = \sqrt{\text{TVAR}}$; $\tau_0 = 0.001$ s	$(0.08 \times 10^{-12}\tau^{-1/2} + 40 \times 10^{-15})$ ps
Calibration repeatability error (RMS)	1.5 ps
Harmonic in the reference signals	<60 dBC

Table 4. Characteristics of the detection chain.

Detection diameter of the non-linear detection	21 µm
Detection diameter of the linear detection	250 µm
Field of view	55.1°
Geometrical uncertainty of the equivalent detection point	<1 mm
Pulsed threshold detection @ detection probability = 5%	0.3 µJ m^{-2}
Pulsed energy absolute maximum rating	0.01 J m^{-2}
Pulsed energy dynamic (orders of magnitude)	4
CW minimum threshold	0.25 W m^{-2}

by an active circuit triggered by the linear detection a few nanoseconds before the expected arrival of the laser pulses and brought back to its 'off'-state as soon the detection (and thus avalanche) occurs. The linear detection is made with a classical avalanche photodiode associated with a high-speed comparator for the quenching circuit and two analogue to digital converter chains for the laser energy and sunlight measurements.

Each photodetection channel includes the following.

- A collimation optic to fit the necessary field of view to each photodetector.
- A neutral density filter with radially variable transmission to minimize the noise and to reduce the dynamical variations of the laser energy.
- A pinhole to limit the field of view to the angular extent of the whole Earth.
- A spectral filter at 532.1 nm to improve the signal-to-noise ratio.

The collimation optics of the non-linear photodetection forms an equivalent geometric point of detection which is located on the main axis of the optic module. Time stampings of the all the laser events are referenced to this point which is invariant for the T2L2 instrument whatever the incident angle of the laser beam. The time tagging of the laser pulses coming from the Earth is always made as compared with this equivalent detection point.

The main parameters of the whole detection chain were deduced from several experiments made both before and during integration of the T2L2 space instrument on the Jason 2 satellite. These parameters are summarized in table 4. Some measurements were made directly on the individual detection modules (disconnected from the main T2L2 instrument) while others were conducted on the whole instrument.

Many parameters were compared with the theoretically expected value in order to validate the realization of the instrument. Among them, one parameter is not in conformity: the optical coupling of the non-linear detection was measured 80% smaller than the expected value. The main consequence of that defect is the real number of photons used for the non-linear detection and the final repeatability error for low-energy level. Since the triggering of the detection is imposed by the linear detection, this defect does not directly impact the overall detection threshold.

Table 5. Characteristic of the chronometer; the time deviation @ 1 s is computed from the complete T2L2 instrument internally connected to the DORIS oscillator.

Repeatability error @ minimum energy (RMS)	70 ps
Repeatability error @ mid-scale energy (RMS)	10 ps
Residual time walk over the whole dynamic of incident angle	35 ps
Time deviation $\sigma_x = \sqrt{\text{TVAR}}$ @ 1 s	2 ps

3.6. Chronometry

The chronometry performance of the whole metrology chain is imposed by the characteristics of both the event timer and the detection. Experiments were carried out to evaluate the parameters as a function of the energy per pulse and some others by evaluating the characteristics as a function of incident angle (attitude). Table 5 summarizes the main parameters. As compared with the expected results at low-energy level, the repeatability error is two times greater. This is due to the bad coupling on the non-linear detection chain (described above) which gives a smaller photon number and generates a spot size larger than the photodiode.

The optical transmissions of each channel (linear and non-linear) are not exactly the same on the whole dynamic range of the incident angles ρ. As a consequence, the photon number received on the non-linear channel and evaluated by the linear one is not accurate and depends on ρ. Due to the time walk of the non-linear photodiode, the overall chronometry is impacted by an error depending on ρ.

4. T2L2 modelling of the flight instrument

Going from T2L2 raw acquisitions to picosecond dates requires applying several corrections to the data at different levels.

- The corrections dealing with the time tagging: they are of two kinds, those that depend only on the instrument (section 4.1) and those where one needs to identify the laser station to take into account the geometry (sections 4.2, 4.3 and 4.4). The former are applied automatically during ground processing and are transparent for the user. The latter are executed by the T2L2 Scientific Mission Centre [17] to produce regular time transfer.

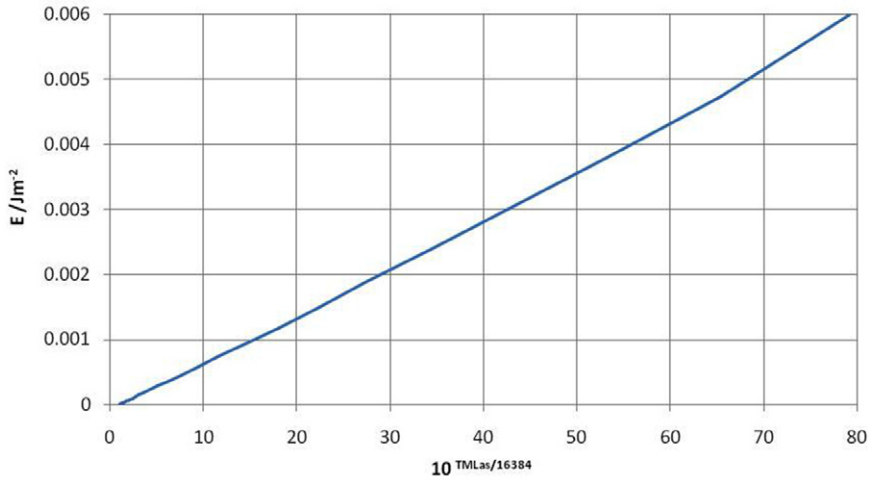

Figure 6. Correspondence between T2L2 measurement and energy density flux.

Table 6. Polynomial coeffficient of the F_{PDAC} function.

Order	0	1	2	3	4	5	6	7	8	9
$\times 10^{-6}$	−69.76	68.002	0.3984	-3.564×10^{-2}	-4.752×10^{-4}	1.9146×10^{-4}	-9.010×10^{-6}	1.8528×10^{-7}	-1.800×10^{-9}	6.7441×10^{-12}

– The corrections dealing with ranging: they are necessary to take into account the geometry of both the reflection and detection points (sections 4.5 and 4.6).
– The optimization of T2L2 operation in order to adjust the level of noise with respect of the sun Albedo (sections 4.7 and 4.8).
– The elaboration of a continuous and accurate on-board time scale to take into account the behaviour of the on-board clock (section 4.9).

4.1. Event timer

With a repeatability error of 2.5 ps RMS and a global linearity better than 1 ps, the event timer can be considered as a perfect instrument as compared with characteristics of other subsystems. To obtain this performance, the event timer realizes every 1 s an internal calibration which permits one to give the time drift of the timer and the variation of some internal reference signals. This is done through some reference pulses generated internally. These calibration data are sent to the Instrument Mission Centre together with data corresponding to laser pulse time tagging whereupon the centre performs the global data reduction.

4.2. Pulsed laser energy flux measurement

The T2L2 space instrument gives an individual measure of the energy for each pulse detected. The measurements are conducted over an energy dynamic range of four orders of magnitude. The result is digitized on 15 bits scale ($\mathrm{TM_{Las}}$). The response of the instrument is pre-linearized by a logarithmic law f_{PDAC} (figure 6):

$$E_{\mathrm{Puls}} = f_{\mathrm{PDAC}}\left(10^{\frac{\mathrm{TM_{Las}}}{2^{14}}}\right). \quad (1)$$

This law can be approximated by a simple polynomial law of order 9 to cover the whole dynamic of the instrument (table 6).

The residual of that law over the whole dynamic is smaller than $10\,\mu\mathrm{J\,m^{-2}}$.

4.3. Time-walk versus energy compensation

The time-walk compensation is applied to the raw timing event of the T2L2 space instrument to take into account the time shift induced by the photon number variation. It is deduced from measurements made with the reference event timer and the control of the laser energy (see section 3.5). The timing events of T2L2 are compared with those coming from the reference with a variable energy. The laser energy is controlled and measured during the process. The incident angle of the laser beam is 0° (figure 7).

The time-walk can be fitted with a polynomial law of order 9 having the coefficients, as given in table 7.

4.4. Time-walk versus attitude compensation

As described above, the overall chronometry is degraded if the energy measured by the linear detection is different from the energy received by the non-linear channel. The transmission of each channel has been designed to be identical. In practice, there is a substantial difference which generates a chronometry dependence as a function of ρ (due to the time walk of the non-linear photodiode). If this dependence is identified and if the attitude of satellite is known, one can apply *a posteriori* attitude correction to solve this dependence. The stellar sensors of the Jason 2 attitude control system deliver the attitude with an accuracy better than 0.1° that permits to compute ρ with the same level of accuracy. Figure 8 is an illustration of the energy variation, the corresponding time walk induced by this

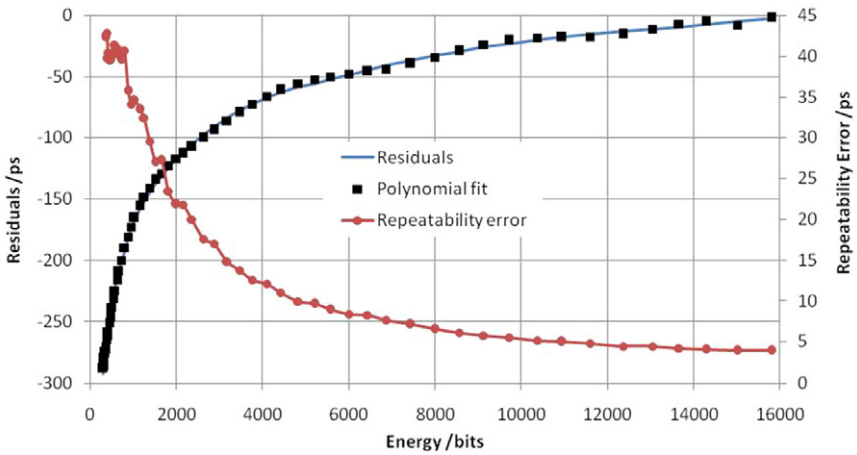

Figure 7. Time walk and repeatability error as a function of laser energy. The difference between the polynomial fit and the time walk is 3 ps RMS.

Table 7. Time-walk compensation law versus measured energy.

Order	0	1	2	3	4	5	6	7	8	9
	−395.9	0.4425	-3.212×10^{-4}	1.3496×10^{-7}	-3.367×10^{-11}	5.1483×10^{-15}	-4.861×10^{-19}	2.7614×10^{-23}	-8.640×10^{-28}	1.1433×10^{-32}

energy variation and the compensated chronometry computed with the polynomial law presented in table 7. The final attitude correction to be determined is the residual of that compensated chronometry. It can be fitted with a polynomial law of order 4 (table 8).

Using the energy time-walk correction together with this attitude model gives a residual over the whole field of view of 3 ps RMS.

4.5. Reflection function

The laser pulse reflection is used to evaluate the time of flight between the Earth and the satellite. The employed reflector array (LRA) is formed of a pyramidal unit consisting of one central corner at the top and height corner cubes on the periphery having an angle of 50° as compared with the central corner cube. Each corner cube is made of Suprasil quartz and has a diameter of 31.75 mm.

Because the equivalent reflection point of each corner cube of the pyramidal is not located at the same place, the timing model of the reflection function depends on the incident angle ρ. The global reflected pulses are affected by a specific time signature coming from the superposition of the pulses reflected by each individual of the corner cubes. Due to the geometry of the pyramidal, the maximum time dispersion in the worst case is 25 ps.

Further, the real time error for the two-way laser ranging depends on the detection type used by the respective laser station. Some stations use a compensated photodetection (CSPAD) which introduces a time delay depending on the optical signature of the pulses. Some stations use a single photodetection (SPAD) capable (in principle) to reproduce the shape of the optical signature and some other stations use a linear detector (MCP) which generates an analogue signal also affected by the optical signature. Given this diversity of detection and to simplify the restitution of the range, it has been decided to consider the LRA as a perfect target having a unique reflection point located on the main axis of the pyramidal, 20.5 mm above the mechanical interface plane.

4.6. Geometry

Because LRA and detection unit are not located at the same place, the reflection and detection points do not coincide. It is therefore necessary to compute, for each echo obtained, the projected distance between these points. This calculation is performed from the position of both the laser station and the satellite and from the attitude of the satellite. We use the local rectangular coordinates of the reflection and detection points in the satellite reference frame. These are given with an accuracy better than 1 mm. Thanks to the fixed vector LRA-T2L2 and to a set of quaternions that precisely ($\pm 0.1^\circ$) represents the change of frame between the satellite body and the inertial frame, we compute the geometrical correction for all laser events. The overall uncertainty of this correction is expected to be 3 ps.

4.7. Background optical power flux measurement

The instrument was calibrated to measure a DC optical power flux in two distinct configurations. The first one corresponds to a collimated beam and the second one to a diffused emission. The first measurement is suited to measure optical flux coming from a ground DC laser (which could be planned for some link budget experiment) and the second is suited to measure the global solar flux back scattered by the earth. This diffused measurement permits to compute the Earth emittance and albedo. Both measurements are carried out at 532.1 nm with a spectral bandwidth of 10 nm.

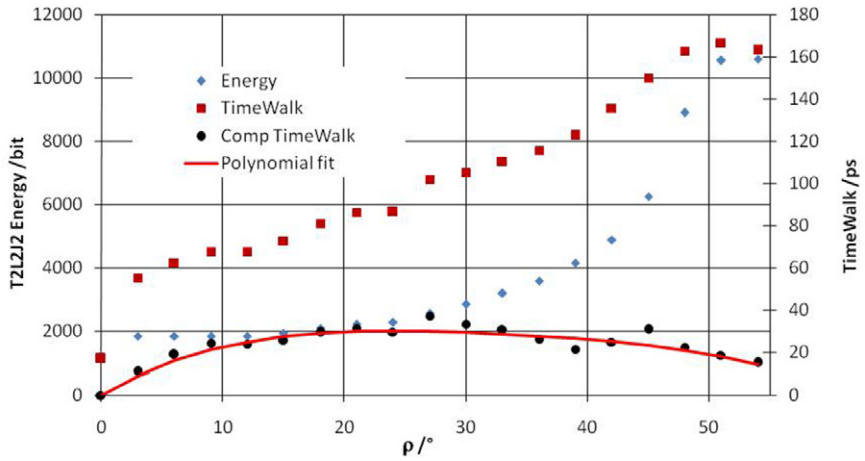

Figure 8. Energy variation on the non-linear detection corresponding to the time walk induced by this energy variation and the compensated chronometry. The difference between the polynomial fit and the time walk is 3 ps RMS.

Table 8. Chronometry compensation as a function of incident angle ρ.

Order	0	1	2	3	4
	0	3.406	−0.1378	0.002 431	$-1.771\,66 \times 10^{-5}$

Table 9. Threshold condition for three distinct operation conditions.

Condition	Threshold P_{CW}/W m^{-2}	Min energy/μJ m^{-2}
Night	0	0.7
Day	0.5	10
Sun	28	35

Both measurements are referred to the measurement of the linear photodetector expressed in volts. The correspondence law between measurement in bits (TM_{CW}) and measurement in volts is

$$U_{CW} = (TM_{CW}/32\,768 - 1) \times 1.024 + 0.002 - ((32\,800/32\,768 - 1) \times 1.024 + 0.002)\,. \quad (2)$$

The conversion function doing the correspondence between U_{CW} and the optical power flux (W m^{-2}) with a collimated beam having an incidence angle equal to 0° is given by

$$P_{CW} = 157 U_{CW}. \quad (3)$$

The Earth emittance M_t is given by

$$M_t = (157 U_{CW} T_0)\,/I, \quad (4)$$

where $T_0 = 0.041$ is the optical transmission of the linear detection chain for an incidence angle equal to 0° and $I = 0.2$ the geometrical integral of the whole optic over the global field of view of the instrument.

The albedo measurement is based on the knowledge of the solar emittance M_{SF} through the spectral transmission of the T2L2 instrument. M_{SF} is computed from the transmission of the spectral filter (FWHM = 10 nm), from the attenuation generated by the lenses and from the solar spectrum. The albedo is given by

$$Al = (157 U_{CW} T_0)\,/\,(M_{SF} I)\,, \quad (5)$$

with $M_{SF} = 19$ W m^{-2}.

4.8. Threshold detection

In order to minimize the number of false detections and to maximize the detection capability, the threshold detection of the linear channel is adjusted as a function of the solar flux back scattered by the Earth. This process is automatically programmed from the ground. Inside the instrument, the main adverse effect produced by a threshold change is the time delay variation between the Geiger pulse and the laser event. This can generate a voltage polarization variation and finally a transit time evolution of the non-linear detection. Some preliminary measurements have shown that a possible chronometry sensitivity was not measurable for variations smaller than 10% as compared with the whole dynamic. The solar flux is measured by the CW channel of the linear detection. Figure 9 is a typical observation of that CW power over a complete revolution of Jason 2.

Some preliminary tests during the first months after the launch have allowed to set three distinct operation conditions (table 9). The first one concerns the night period. The threshold is set to be just above the electronic noise of the detection. The second one is the day condition where the threshold is set to produce a noise rate below 1 Hz. It corresponds to a measured power $P_{CW} = 0.5$ W m^{-2}. The last one is the case where the sun is inside the field of view of the instrument.

4.9. Local oscillator

The two most important sensitivities of the DORIS oscillator are temperature and radiation. The DORIS instrument gives a complete monitoring of the oscillator temperature and two passenger instruments on-board Jason 2 are devoted to radiation measurements. In principle, the measurements of temperature and radiation could permit one to improve the long-term oscillator stability but up to now, it has not been possible to establish a satisfying model. For temperature, thermal gradient and temporal phase shift would probably

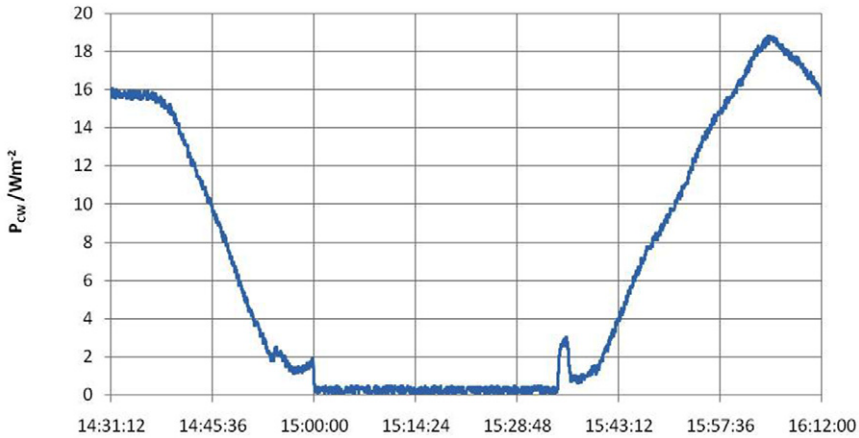

Figure 9. Typical measurement of the solar flux backscattered by the Earth over a complete orbit of Jason 2. The situation where the power is close to 0 corresponds to the satellite-level eclipse. The little peaks before and after the eclipse is due to the sunrise and to the sunset even if the Sun is not visible through the field of view.

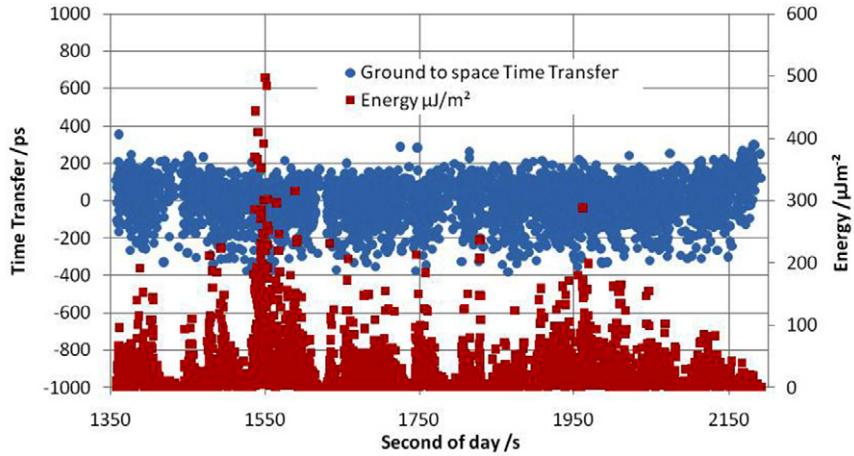

Figure 10. Ground to space time transfer and energy.

imply a model taking into account a subtle response as a function of time and temperature.

For irradiation, even if we can deduce from laboratory measurements a global trend, the real behaviour is much more complex. Some hysteresis and some cure phenomena limit our capability to apply a consistent frequency correction.

Ageing is the most important long-term sensitivity of the oscillator (table 1). Because ageing depends also on many external parameters, such as time, temperature or radiation, it has to be determined over small period over time transfer comparison through some accurate ground clocks. This can be achieved for extrapolation and interpolation. Due to the frequency evolution of the DORIS oscillator, the order of magnitude of time drift over the whole mission duration ($\geqslant$2000 days) changed between 20 ns s^{-1} to 45 ns s^{-1}.

5. Ground to space time transfer example

Disposing over the whole set of correction data, one may generate an *a posteriori* time transfer from a laser station to the satellite and thus to another laser station.

Figures 10, 11 and 12 illustrate a typical ground to space time transfer. It was obtained on 12 April 2014 with the MeO Station at Observatoire de la Côte d'Azur, France. The MeO station is based on a 1.54 m telescope, a mode-locked Nd : YAG laser (pulse width 100 ps) and a hydrogen maser as time reference. Figure 10 gives the difference between the hydrogen maser and the DORIS oscillator. A frequency correction of -43.314×10^{-9} has been applied to the frequency of the DORIS oscillator to take into account the frequency offset and the ageing of the oscillator (section 4.9). The figure also gives the energy received in the plane of the satellite of each laser event detected (section 4.2). The short-term energy variation is induced by the atmosphere while the long-term variation is generated by the pointing errors. Both the time walk versus energy (section 4.3) and the time walk versus attitude (section 4.4) have been taken into account in these data reduction.

Figure 11 shows the dependence between received energy and the time walk which is deduced from the difference between ground and space clocks. One can observe that the time walk versus energy (section 4.3) is correctly taken into account because the dots are symmetrically centred around zero.

Figure 12 gives the time of flight from which one deduces the propagation delay of the time transfer and gives also

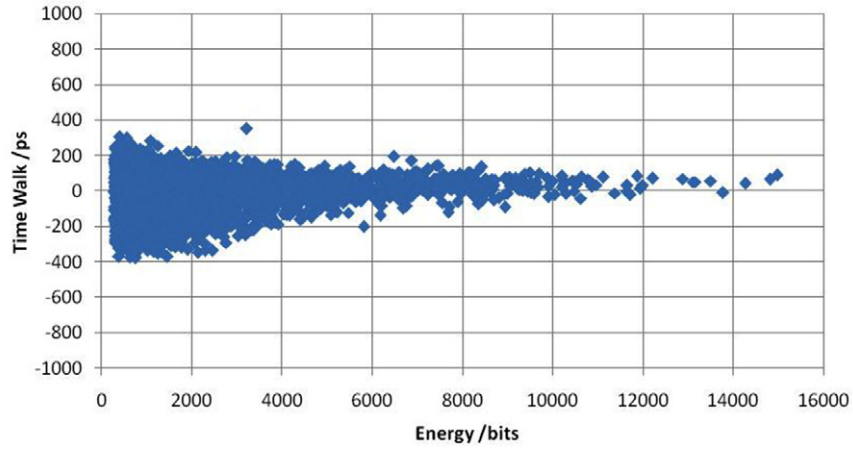

Figure 11. Time walk as a function of the energy received.

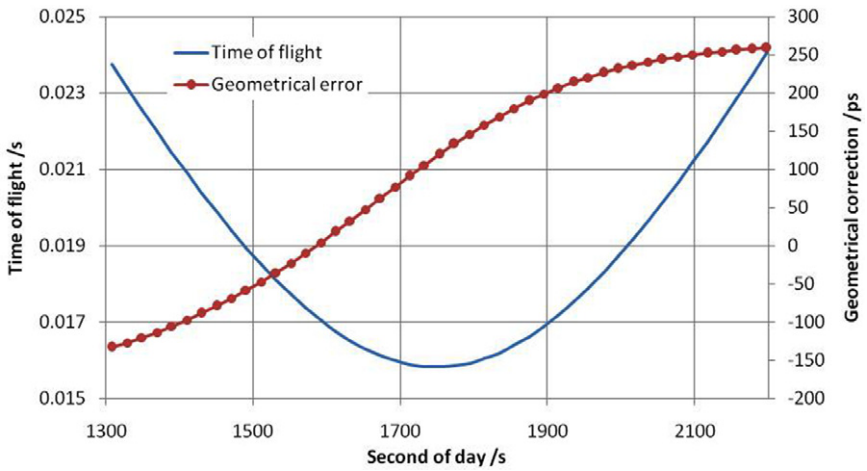

Figure 12. Time of flight (propagation delay between ground station and space segment during the satellite pass) and geometrical correction of reflector position to detector position.

the geometrical correction (section 4.6) permitting to take into account the difference between the corner cubes and the detection module. It illustrates the magnitude of implied corrections.

6. Conclusions—perspectives

The paper gives a global description of the T2L2 flight instrument and a precise summary of all the timing contributions from the sub-elements of the instrument. It also gives a complete report of the experimental setup which has been built to characterize the instrument. It includes the measurement method and the performance of the benches. The timing model of T2L2 flight instrument is fundamentally used to process the data in order to be able to generate the best possible time transfer. The model is used by the T2L2 Scientific Mission Centre which produces regular time transfer of all laser stations with involved clocks participating to the project. The aim of the paper is to give to the final user the information needed to understand how the time transfer is processed. Users should use the model to process by themselves raw data in order to compare and to improve the final time transfer. The experimental characterization of the instrument performed in this study will also be used in the near future to improve our knowledge on optical link budgets. This will be done through several experiments based on some precise characterization of the atmosphere together with some measurements of the laser energy emitted from ground and received on-board. Some complementary studies should also permit to improve the model of the on-board oscillator which is crucial for time transfers in non-common view mode.

References

[1] Fridelance P, Samain E and Veillet C 1997 T2L2—Time Transfer by Laser Link: a new optical time transfer generation *Exp. Astron.* **7** 191–207
[2] Samain E and Fridelance P 1998 Time Transfer by Laser Link (T2L2) experiment on MIR *Metrologia* **35** 151–9
[3] Samain E *et al* 2011 Time Transfer by Laser Link—T2L2: current status and future experiments *Proc. European Frequency and Time Forum (San Francisco, CA)* pp 378–83
[4] Samain E *et al* 2008 T2L2 experiment on Jason 2 and further experiments *Int. J. Mod. Phys.* D **17** 1043–54
[5] Samain E, Vrancken P, Weick J and Guillemot P 2007 T2L2 flight model metrological performances *Proc. IEEE Frequency Control Symp. Joint with the 21st European Frequency and Time Forum (Geneva, Switzerland)* pp 1291–4

[6] Vrancken P 2008 Characterization of T2L2 (Time Transfer by Laser Link) on the Jason 2 ocean altimetry satellite and Micrometric laser ranging *PhD Thesis* Université de Nice Sophia-Antipolis, Online resource: http://tel.archives-ouvertes.fr/tel-00367703

[7] Auriol A and Tourain C 2010 DORIS system: the new age *Adv. Space Res.* **46** 1484–96

[8] Samain E and Guillemot P 2014 T2L2 optical design of the space segment *J. Opt.* submitted

[9] Samain E and Dalla R 2002 Time walk compensation of an avalanche photo-diode with a linear photo-detection *Proc. 13th Int. Laser Ranging Workshop (Washington, DC)*

[10] Samain E 1998 Timing of optical pulses by photodiode in Geiger mode *Appl. Opt.* **37** 502–6

[11] Zelensky N, Berthias J and Lemoine F 2006 DORIS time bias estimated using Jason-1, TOPEX/Poseidon and ENVISAT orbits *J. Geod.* **80** 497–506

[12] Lemoine J M *et al* 2006 A corrective model for Jason-1 DORIS Doppler data in relation to the South Atlantic Anomaly *J. Geod.* **80** 507–23

[13] Vrancken P, Samain E, Weick J and Guillemot P 2007 The T2L2 metrological test bed *Proc. IEEE Frequency Control Symp. Joint with the 21st European Frequency and Time Forum (Geneva, Switzerland)* pp 307–11

[14] Prochazka I, Hamal K and Sopko B 2004 Recent achievements in single photon detectors and their applications *J. Mod. Opt.* **51** 1289–313

[15] Prochazka I, Hamal K and Kral L 2007 Single photon counting module for space applications *J. Mod. Opt.* **54** 151–62

[16] Candelier V *et al* 2001 Recent progress in ultra-stable oscillators for space on-board and ground applications *Proc. EFTF* pp 325–31

[17] Exertier P 2014 Time Transfer by Laser Link: validation of analysis *Metrologia* submitted